

Absolute $O_2(a^1\Delta)$ Concentration Measurement in Singlet Oxygen Generator by Using the Piston Source Method

Liping Duo,* Tiejie Cui, Zengqiang Wang, Wenwu Chen, Bailing Yang, and Fengting Sang

Short Wavelength Chemical Laser Laboratory, Dalian Institute of Chemical Physics,
Chinese Academy of Sciences, Dalian 116023, China

Received: March 17, 2000; In Final Form: October 26, 2000

A calibrated piston source of light, which simulates a cylindrical-volume luminosity source, has been used to measure the absolute concentration of $O_2(a^1\Delta)$. It is proved that this piston source method is one of the simplest and most convenient ways to measure the $O_2(a^1\Delta)$ concentration in a singlet oxygen generator, especially in real time measurements. Discussions about the method and the results are also given.

Introduction

As the shortest-wavelength chemical laser and the only laser based on electronic transitions, the chemical oxygen–iodine laser (COIL) is of great interest owing to its potential applications in both industrial and military fields. As the energy source of the laser, the singlet oxygen generator (SOG) is a key part of the COIL, and consequently, the yield of $O_2(a^1\Delta)$ in the SOG is an important parameter for chemical efficiency.

Various methods have been developed to measure the concentration of $O_2(a^1\Delta)$, such as electron paramagnetic resonance (EPR),¹ photoionization,² isothermal calorimetry,³ absorption measurements of ground-state oxygen,^{4–6} measurement of the $1.27\ \mu\text{m}$ emission intensity,⁷ etc. Conventionally, due to its simplicity, the method most commonly employed is the last of the above-mentioned techniques. However, with this method it is very difficult to calibrate for high-pressure operations, while the EPR method has been successfully used for calibrations in lower-pressure operations. More recently, the spontaneous Raman imaging⁸ method has been developed and used for the direct measurement of the $O_2(a^1\Delta)$ yield, but the measuring system is too costly for most laboratories.

In this paper, we used the piston source (PS) method, which is basically a simulation of the cylindrical-volume luminosity source for absolute measurements and which has been successfully used to measure the reaction rates of NO and O_2 ,⁹ to measure for the first time the absolute concentration of $O_2(a^1\Delta)$ in SOG. Finally, discussions about the method and the results are also presented.

Experiment and Principle

The emission tube and optical measuring system of the PS method are shown schematically in Figure 1. Inside the dashed rectangle of Figure 1 the measurement setup of the PS method is schematically indicated, while outside this dashed rectangle the Jet SOG, the diagnostic zone and the pumping system are illustrated. The cylindrical stainless steel tube, connected with a diagnostic tube of the Jet SOG, had an internal diameter of 40 mm and a length of 300 mm. The entrance and the exit ports

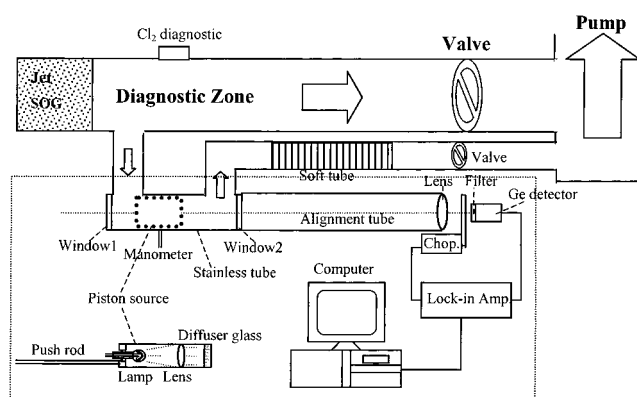


Figure 1. Schematic chart of the setup for the measurement of absolute concentration of $O_2(a^1\Delta)$ by the PS method.

for gases were 40 mm in diameter. Gases flowed through the tube at linear speeds higher than 150 m/s. In the middle of the tube, there was a capacitance manometer. The detecting system included a lens, a filter at the center of $1.27\ \mu\text{m}$ with bandwidth of 23 nm, a chopper, and a cooled Ge detector which was located 540 mm from window 2, i.e., the nearer end of the stainless steel tube and on the tube axis. The signals were amplified by a lock-in amplifier and recorded by a computer.

$O_2(a^1\Delta)$ was produced by gaseous chlorine and BHP liquid in the Jet SOG and then flowed through the stainless steel tube, emitting $1.27\ \mu\text{m}$ photons for all space within a 4π solid angle. But the detecting system only collects emissions at a certain solid angle, which is very difficult to calculate for a volume-luminosity source. Assuming that the volume luminosity is composed of numerous luminous elements, it is impossible to know how much of each element contributes to the detected intensity, especially for the off-axis luminous elements. Therefore, the absolute $O_2(a^1\Delta)$ concentrations are difficult to obtain, though the photon number corresponding to the emission intensity can be known. So the $1.27\ \mu\text{m}$ emission intensity method is generally a relative measurement.

On the basis of the calibrated PS method, the above difficulties can be avoided. The schematic of the piston source (PS) structure can be seen in the zoom of Figure 1. A small lamp

* Corresponding author. Email: dlp@dicp.ac.cn. Tel: 86-411-4671991, ext. 843. Fax: 86-411-4679766. Postal address: P. O. Box 110, Dalian, 116023, China.

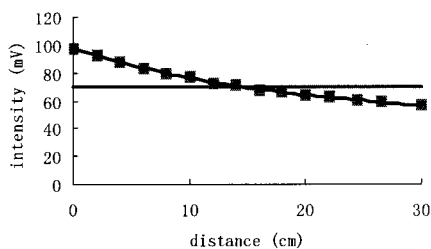


Figure 2. Signal intensity as a function of the piston source position.

is located at the focusing point of a lens, in front of which a ground-glass plate is added to make the light diffuse. The brightness of the PS is known (details are presented in the appendix) as

$$B_{\text{PS}} = B_{\text{st}} \frac{S_{\text{PS}}}{S_{\text{st}}} \frac{A_1}{A_{\text{PS}}} \frac{a^2}{L^2} \quad (1)$$

where, B_{PS} denotes the brightness of the PS ($\text{W cm}^{-2} \text{nm}^{-1} \text{str}^{-1}$), B_{st} is the brightness of the standard tungsten lamp at 1270 nm ($\text{W cm}^{-2} \text{nm}^{-1} \text{str}^{-1}$), S_{PS} denotes the detected signal for the PS at a distance a from the system detector (mV), S_{st} is the detected signal for the standard tungsten lamp at a distance L from the system detector (mV), A_1 is the luminous area of the standard tungsten lamp (cm^2), L is the distance of the tungsten lamp from the collecting lens (m), A_{PS} is the area of the diffuser of the PS (cm^2), and a is the distance of the diffuser of the PS from the collecting lens (m).

1. Solid Angle of the Volume-Luminosity Source and the Sensitivity of the Detecting System. For calibrating the cylindrical-volume luminosity, we remove window 1 and put the PS into the tube (see Figure 1). As a unit part, PS can be moved smoothly in the stainless steel tube. Presuming the position of window 2 as the zero point, we pull the PS along the tube and record the signal at different positions. In this way, the profile of simulation for the cylindrical-volume luminosity source can be obtained (shown in Figure 2). The integration of the signal along the length of the tube equals to the signal emitted from the cylindrical-volume luminosity, since the moving disk source at different positions corresponds to the luminous elements of the cylindrical-volume luminosity. Herein, we keep the current of the lamp identical with the PS brightness calibration

$$S_{\text{PS}}^{\text{V}} = S_{\text{PS}}' l \quad (2)$$

where, S_{PS}^{V} means the integration of the signal along the distance of the tube, S_{PS}' is the average signal of the integration, and l denotes the length of the tube.

Thus, the luminous disk of which brightness increases by l times at the average position could be treated as an equivalent of the cylindrical-volume luminosity. They have the same solid angle, written as θ_{real} . Then the photon flow rate denoted as P_{PS} and collected by the detector can be expressed as follows:

$$P_{\text{PS}} = (I B_{\text{PS}}) A_{\text{PS}} \Delta \lambda \left(\frac{\lambda}{hc} \right) \theta_{\text{real}} \quad (3)$$

where, P_{PS} is the photon flow rate of the PS located at the average position (in photons s^{-1}), $\Delta \lambda$ is the bandwidth of the filter used in the detecting system (in nm), λ is the wavelength of photons emitted from $\text{O}_2(\text{a}^1\Delta)$ (1270 nm), h is the Planck constant, c is the speed of light, and θ_{real} is the solid angle for the cylindrical-volume luminosity source.

The sensitivity of the detecting system, written as ξ_{PS} , is

$$\xi_{\text{PS}} = \frac{P_{\text{PS}}}{S_{\text{PS}}^{\text{V}}} = \frac{B_{\text{PS}}}{S_{\text{PS}}'} A_{\text{PS}} \Delta \lambda \left(\frac{\lambda}{hc} \right) \theta_{\text{real}} \quad (4)$$

Putting formula 1 into 4, we get

$$\xi_{\text{PS}} = B_{\text{st}} A_1 \Delta \lambda \left(\frac{\lambda}{hc} \right) \theta_{\text{real}} \left(\frac{S_{\text{PS}}}{S_{\text{st}}} \right) \left(\frac{1}{S_{\text{PS}}'} \right) \left(\frac{a^2}{L^2} \right) \quad (4')$$

2. Photon Flow Rate and the Absolute $\text{O}_2(\text{a}^1\Delta)$ Concentration. Having finished the calibration, we remove the PS and fasten window 1. When the gas exited from the Jet SOG and flowed into the cylindrical opaque tube, $\text{O}_2(\text{a}^1\Delta)$ emission signal could then be detected. The signal corresponds to photons collected at the solid angle of θ_{real} for an $\text{O}_2(\text{a}^1\Delta)$ cylindrical-volume luminosity source. Thus, the photon emission rate at all space solid angles of 4π can be written as

$$p_{\text{v}} = \xi_{\text{PS}} S_{\text{v}} \left(\frac{4\pi}{\theta_{\text{real}}} \right) \quad (5)$$

where, p_{v} is the photon flow rate (photon/sec) and S_{v} is the detecte signal of $\text{O}_2(\text{a}^1\Delta)$ emission in the stainless steel tube (mV). Introducing formula 4' into formula 5, we have

$$p_{\text{v}} = 4\pi B_{\text{st}} A_1 \Delta \lambda \left(\frac{\lambda}{hc} \right) \left(\frac{S_{\text{PS}}}{S_{\text{st}}} \right) \left(\frac{S_{\text{v}}}{S_{\text{PS}}'} \right) \left(\frac{a^2}{L^2} \right) \quad (6)$$

If

$$I_{\text{st}} = B_{\text{st}} A_1 \Delta \lambda \left(\frac{\lambda}{hc} \right) \quad (7)$$

then

$$p_{\text{v}} = 4\pi I_{\text{st}} \frac{S_{\text{v}}}{S_{\text{PS}}'} \frac{S_{\text{PS}}}{S_{\text{st}}} \frac{a^2}{L^2} \quad (8)$$

where, I_{st} is the photon emission rate per cubic angle at a specific wavelength of the standard Tungsten lamp (photons $\text{s}^{-1} \text{str}^{-1}$). When $a = L$, then formula 8 is the same as that in ref 9 and is as follows:

$$p_{\text{v}} = 4\pi I_{\text{st}} \frac{S_{\text{PS}}}{S_{\text{PS}}'} \frac{S_{\text{v}}}{S_{\text{st}}} \quad (9)$$

The advantage of the PS method is that the complicated solid angle for a cylindrical-volume luminosity source can be accounted for and uncertainties in the PS parameters are minimized.

Then we can obtain the $\text{O}_2(\text{a}^1\Delta)$ concentration as

$$[\text{O}_2(\text{a}^1\Delta)] = \frac{p_{\text{v}}}{VA} \quad (10)$$

where, A is the coefficient of Einstein spontaneous emission ($2.31 \times 10^{-4} \text{s}^{-1}$)⁷ and V is the volumetric value of the stainless steel tube.

This experimental technique for the measurement of the absolute concentration of $\text{O}_2(\text{a}^1\Delta)$ eliminates the need of

TABLE 1: Calibrated Parameters

I_{st} (photon s ⁻¹ str ⁻¹) at 1.268μm	4.902 × 10 ¹⁷
S_{st} (mV)	219.0
S'_{PS} (mV)	16.30
S''_{PS} (mV)	69.90

mathematical integration⁷ and thereby improves the accuracy of the optical measurements.

Results and Discussion

The mean position derived from the profile shown in Figure 2 was 14.3 cm. The calibrated parameters are listed in Table 1.

On the basis of these calibrated parameters as well as formulas 8 and 10, the concentration O₂(a¹Δ) can be derived as

$$[O_2(a^1\Delta)] = 1.100 \times 10^{15} S_v \text{ (photons cm}^{-3}\text{)} \quad (11)$$

When the temperature is 273K, the partial pressure of O₂(a¹Δ) can be obtained as

$$P_{O_2(a^1\Delta)} = 0.03107 S_v \text{ (Torr)} \quad (12)$$

The yield of O₂(a¹Δ), which means a percentage of [O₂(a¹Δ)] in the total oxygen, is an important parameter for a SOG. By knowing the flow rate ratios of He and Cl₂, the utility of chlorine, the total pressure, and the water vapor partial pressure in a SOG, we can get the yield of O₂(a¹Δ) from the following formula:¹⁰

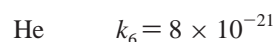
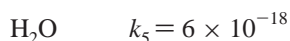
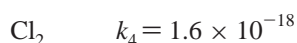
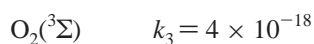
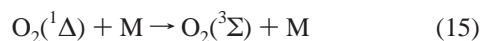
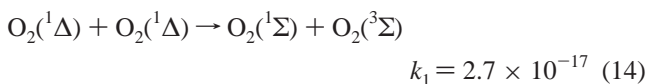
$$\text{yield} = \frac{[O_2(a^1\Delta)]}{(P_t - P_{H_2O})U_{Cl_2}N + 1} \quad (13)$$

where N is the flow rate ratio of He and Cl₂, P_t is the total pressure, P_{H_2O} is the water vapor partial pressure (it is about 2 Torr), and U_{Cl_2} is the utility of chlorine.

According to formulas 12 and 13, a series of experimental results are obtained as shown in Table 2.

From Table 2, we can see that most of the yields of O₂(a¹Δ) of the Jet SOG are above 50%. However, it is worth of mentioning that several points have to be considered by using the PS method to measure the absolute concentration of O₂(a¹Δ) in SOG.

1. Quenching of O₂(a¹Δ) by Gaseous Species. The O₂(a¹Δ) quenching reaction by the gaseous species, such as O₂(¹Δ), O₂(¹Σ), O₂(³Σ), Cl₂, H₂O, He, and H₂O₂ at the exit of the SOG, are as follows:



The unit of these reaction rates is cm³ molecules⁻¹ s⁻¹.

TABLE 2: A Series of Experimental Results

exp. no.	S_v (mV)	P_t (Torr)	N	U_{Cl_2}	$P_{O_2(a^1\Delta)}$ (Torr)	yield
71001	64	28	3.94	0.77	2.0	0.50
71002	71	27	4.00	0.69	2.2	0.65
71003	74	27	4.23	0.69	2.3	0.71
71004	67	26	4.03	0.65	2.1	0.68
71005	66	26	4.15	0.62	2.0	0.72
71006	64	25	4.11	0.63	2.0	0.71
71007	64	28	4.36	0.57	2.0	0.73
71008	60	27	4.30	0.62	1.9	0.65
71009	62	25	4.53	0.57	1.9	0.83

The saturated vapor of H₂O₂ is only 1/20 of that of H₂O at the same temperature, and furthermore, its quenching rate is nearly zero, so the quenching by H₂O₂ is negligible. The quenching by He is 3 to 4 orders of magnitude less than that by the other species and can also be neglected. O₂(¹Σ), produced in the transfer of O₂(¹Δ), is normally small owing to quick quenching by H₂O ($k = 6.7 \times 10^{-12}$). So the kinetic equation of O₂(¹Δ) transfer¹⁰ is

$$d[O_2(^1\Delta)]/dt = -[O_2(^1\Delta)]\{(k_1 + k_2)[O_2(^1\Delta)] + k_3[O_2(^3\Sigma)] + k_4[Cl_2] + k_5[H_2O]\} \quad (16)$$

Similarly, the rate of change of the partial pressure can be written as

$$dP_{\Delta}/dt = -P_{\Delta}(1/RT)\{(k_1 + k_2)P_{\Delta} + k_3P_{\Sigma} + k_4P_{Cl_2} + k_5P_{H_2O}\} \quad (17)$$

Assuming that

$$\zeta' = (1/RT)\{(k_1 + k_2)P_{\Delta} + k_3P_{\Sigma} + k_4P_{Cl_2} + k_5P_{H_2O}\} \quad (18)$$

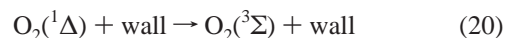
and presuming it is constant during the test (about 8.4 s⁻¹ at the experiments). Integrating formula 17

$$P_{\Delta} = P_{\Delta 0} \exp(-\zeta' t) \quad (19)$$

$P_{\Delta 0}$ is the initial partial pressure of O₂(¹Δ).

When the linear speed of the medium is 200 m/s and the residence time in the tube is 1.5 ms, then [O₂(¹Δ)] at the exit is 98.7% of that at the entrance of the tube. If the linear speed is slower than 150 m/s, the nonuniformity of the cylindrical-volume luminosity source would be obvious, but if it is faster than 150 m/s, it can be negligible. So the linear speed of gases in the stainless steel tube should maintain more than 150 m/s.

2. Quenching of O₂(¹Δ) by the Wall. The quenching rate of O₂(¹Δ) by different materials is not the same, and the kinetic reaction involving the wall is



The quenching coefficient $\zeta' = 2 \times 10^{-5}(v/2R)$ (s⁻¹)¹¹ is adopted for stainless steel. When the linear speed of $v = 200$ m/s and the radius of $R = 2$ cm, $\zeta' = 0.12$ s⁻¹. The quenching percentage of $\zeta = 1.8 \times 10^{-4}$ for $\Delta t = 1.5$ ms can be negligible for quenching by the wall.

3. Gaseous Temperature Effect. O₂(¹Δ) partial pressure, which is calculated from the concentration on the basis of the medium temperature, increases with temperature by 0.015 Torr/K. The yield of O₂(¹Δ) increases by 0.3–0.4%/K. It can be neglected when the change of temperature is not more than 3 K.

4. Effect of the Width of O₂(¹Δ) Emission Profile. The broadening widths of 1.9×10^{-4} cm⁻¹ for pressure and $1.65 \times$

TABLE 3: Relative Errors for [O₂(a¹Δ)]

B_C (%)	5
A_1 (%)	1
$\Delta\lambda$ (%)	5
a^2 (%)	<0.1
L^2 (%)	<0.1
S_{PS} (%)	1
S_{PS}' (%)	1
S_V (%)	1
S_S (%)	1

10⁻² cm⁻¹ for Doppler are all much less than the bandwidth of the filter. Moreover, the emissions of 634, 703, and 762 nm, besides 1270 nm, are all out of the band of the filter. So the effect of the width of O₂(¹Δ) emission profile can be negligible.

5. Uncertainty of the Results. It is also necessary to discuss the relative uncertainties in these values. The uncertainties in the measurements of the O₂(a¹Δ) concentration are due to the uncertainties of the parameters of I_{st} and the four detected voltages. The uncertainty in I_{st} comes mainly from the uncertainty of 5% in the brightness of the standard lamp given by the designer. The uncertainty in the S_{PS}/S_{st} value due to any misalignment of the piston and the standard sources during comparison measurements are negligible at a distance between the source and the detector of more than 100 cm. No misalignment uncertainty in S_V/S_{PS}' need to be considered since the piston source axis is fixed to the axis of the stainless steel tube. The uncertainty in positioning the piston source at its mean of about ±0.5 mm causes a small change in S_{PS}' (see Figure 2). The relative errors of distances a and L of less than 0.1% can be negligible.

According to formulas 8 and 10, the relative errors of the absolute concentration of O₂(¹Δ) are given in Table 3. The total relative error of [O₂(¹Δ)] is ca. 15%.

On the basis of formula 13 the uncertainty in the yield of O₂(a¹Δ) resulted from the uncertainties of the parameters in [O₂(a¹Δ)], P_t , P_{H_2O} , U_{Cl_2} , and the ratio of flow rates of He and Cl₂, which are 15%, 2%, 2%, 5%, and 1%, respectively. So the total relative uncertainty for the yield of O₂(a¹Δ) is ca. 25%.

6. Requirements of the Method in Applications. The piston source method is a simple and compact method for the volume source radiated from long-life emissions. We have to make the cell shorter or the linear speed faster for short-life emissions, but the signal intensity is too weak for a shorter cell, and the speed is limited by the vacuum pump. These requirements may limit this method for general applications.

Conclusion

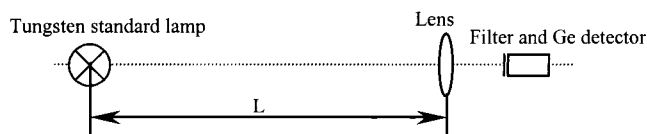
It has been proved that the PS method is one of the simple and convenient ways to measure the O₂(a¹Δ) concentration in SOG, especially in real time measurements.

Acknowledgment. The authors would like to thank Profs. Wang Lin, Ma Yueren, Lu Guosheng, Shao Mingjun, and Liu Yushi for their operating the jet SOG.

Appendix: Calibration of PS Brightness

The PS brightness is calibrated by a standard lamp. Figure 3 is the setup of the calibration system. The system measured the signal of the standard lamp placed at a distance L from the detecting system. The detected photon flow rate is written as

$$P_{st} = B_{st} A_1 \Delta\lambda \left(\frac{\lambda}{hc} \right) \left(\frac{\pi d^2}{4L^2} \right) \quad (a)$$

**Figure 3.** Setup of the calibration system.

So the sensitivity of the detecting system is

$$\xi = P_{st}/S_{st} \quad (b)$$

where P_{st} is the detected photon flow rate for the tungsten standard lamp (photons s⁻¹), B_{st} is the brightness of the standard tungsten lamp at 1270 nm (W cm⁻² nm⁻¹ Str⁻¹), A_1 is the luminous area of the standard tungsten lamp (cm²), L is the distance of the tungsten lamp from the collecting lens (11.626 m), ξ is the sensitivity of the detecting system (photon s⁻¹ mv⁻¹), S_{st} is the detected signal for the standard tungsten lamp at a distance L from the system detector (mv), $(\pi d^2)/(4L^2)$ is the solid angle of the lens for the standard lamp (Str), d is the diameter of the lens (m), $\Delta\lambda$ is the bandwidth of the filter (nm), λ is the center wavelength of the filter (m), h is Planck's constant (6.626×10^{-34} J s), and c is speed of light (3×10^8 m sec⁻¹).

As a unit part, PS instead of the standard lamp was located at the calibration system. The distance is changed to a from the detecting system owing to lower intensity of the PS. The principle is the same as the above:

$$P_{PS} = B_{PS} A_{PS} \Delta\lambda \left(\frac{\lambda}{hc} \right) \left(\frac{\pi d^2}{4a^2} \right) \quad (c)$$

$$\xi = \frac{P_{PS}}{S_{PS}} \quad (d)$$

Hence

$$B_{PS} = B_{st} \left(\frac{S_{PS}}{S_{st}} \right) \left(\frac{A_1}{A_{PS}} \right) \left(\frac{a^2}{L^2} \right) \quad (e)$$

where P_{PS} is the detected photon flow rate for the PS (photons s⁻¹), B_{PS} denotes the brightness of the PS (W cm⁻² nm⁻¹ str⁻¹), S_{PS} denotes the detected signal for the PS at a distance a from the system detector (mv), A_{PS} is the area of the diffuser of the PS (cm²), and a denotes the distance of the diffuser of the PS from the collecting lens (1.405 m).

References and Notes

- (1) Falick, A. M.; Mahan, B. H.; Myers, R. J. *J. Chem. Phys.* **1965**, *42*, 1837.
- (2) Meneal, R. J.; Cook, G. R. *J. Chem. Phys.* **1966**, *45*, 3469.
- (3) Fisk, G. A.; Hays, G. N. *Chem. Phys. Lett.* **1981**, *79*, 331.
- (4) Allen, M. G.; Carleton, K. L.; Davis, S. J. Presented at the 25th AIAA Plasmadynamics and Lasers Conference, Colorado Springs, CO, 1994; AIAA paper 94-2433.
- (5) Kendrick, K. R.; Helms, C. A.; Quillen, B. *SPIE* **1998**, *3268*, 125.
- (6) Xu, Y.; Sheng, X.-Z.; Sun, J.-L.; Bai, J.; Dai, D.; G.; Sha, G.; Xie, J.; Sang, F.; Wang, L.; Duo, L.; Yang, B.; Zhang, C. *SPIE* **1999**, *3612*, 32.
- (7) Kodymova, J.; Spalek, O. *SPIE* **1998**, *3574*.
- (8) Gyls, V. T.; Rubin, L. F. *Appl. Opt.* **1998**, *37*, 1026.
- (9) Woolsey, G. A.; Lee, P. H.; Slafer, W. D. *J. Chem. Phys.* **1977**, *67*, 1220.
- (10) Zhuang, Qi; Sang, F.; Zhou, D. *Short Wavelength Chemical Laser*, 1st ed. (in Chinese); The Publishing House of the National Defense and Industry: Beijing, 1997.
- (11) Avizonic, P. V.; Hason, G.; Truesdell, M. A. *SPIE* **1990**, *1225*, 448.